International Journal of Physical Sciences Vol. 7(20), pp. 2768 - 2774, 23 May, 2012
Available online at http://www.academicjournals.org/IJPS
DOI: 10.5897/IJPS11.1676
ISSN 1992 - 1950 ©2012 Academic Journals

Full Length Research Paper

Synthesis and characterization of hydroxyapatite nanocrystal and gelatin doped with Zn^{2+} and cross linked by glutaraldehyde

Azadeh Rezakhani and M. M. Kashani Motlagh*

Department of Chemistry, Iran University of Science and Technology, Tehran, Iran.

Accepted 07 May, 2012

Different nanocrystals of hydroxyapatite-[HAp]-gelatin [GEL], HAp/GEL/Glutaraldehyde (GA), HAp/GEL/Zn and HAp/GEL/GA/Zn were prepared using the biomimetic process. The nanocrystals were characterized by Scanning Electron Microscopy (SEM), Fourier Transform Infrared Spectroscopy (FTIR) and X-ray diffraction analysis (XRD). The FT-IR spectra of HAp/GEL nanocrystal materials are similar to the spectrum of real bone. Nanocrystals show (002), (222), (211) and (112) planes, which confirm formation of hydroxyapatite phase. Lattice parameters from X-ray diffraction spectra showed that the metal cation was incorporated into the hydroxyapatite structure and has substituted for calcium in the HAp crystal structure and all of the doped HAp formulations were biphasic and crystalline. The hydroxyapatite/gelatin/zinc (HAp/GEL/Zn) composite sintered in 900°C demonstrated that the c-axes of HAp nanocrystals were regularly aligned along collagen fibers.

Key words: Hydroxyapatite, Nanocomposite, Zinc.

INTRODUCTION

Natural bone is a composite material made up of collagen (COL) fiber matrix stiffened by hydroxyapatite(HAp) ($Ca_{10}(PO_4)_6(OH)_2$) crystals that account for 69% of the weight of the bone (Van et al., 1986). The organic phase is composed mainly of a protein, type I collagen (Kalpana 2004). Hydroxyapatite (HAp) is a class of calcium phosphate-based bioceramic, often used as a bone graft substitute owing to its chemical and as bone substitutes having similar biocompatibility and osteoconductivity to bone. The stoichiometric HAp has a chemical composition of $Ca_{10}(PO_4)_6(OH)_2$ with Ca/P ratio of 1.67 (Murugan and Ramakrishna, 2005; Gineste et al., 1999; Sonju Clasen and Ruyter, 1997; Carotenuto et al., 1999). The combination of calcium phosphates and natural or synthetic polymers to develop suitable bone substitutes has been intensively investigated and many researchers have been done to give the biocompatible, bioactive, biodegradable and osteoconductive properties of the natural bone. These composites are being developed with the aim to increase the mechanical scaffold stability and to improve tissue interaction (Itoh et al., 2002).

The practical problems with COL type-I (collagen type-I) are its cost and the poor definition of commercial sources of this material. Therefore in the present study, COL $type^{-1}$ was replaced by a gelatin (GEL) precursor. Gelatin is a natural biopolymer obtained by partial hydrolysis of collagen (Myung et al, 2003).

The HAp-embedded collagen nanostructure has been reproduced through a self-organization reaction of HAp nanocrystals using a biomimetic coprecipitation method (Kikuchi et al., 1999; Chang et al., 2001; Chang et al., 2002), which is based on the idea that biologic systems store and process information at the molecular level (Mann and Ozin, 1996; Stupp and Braun, 1997). To mimic the cross-linkage process in toughening of biological bone, glutaraldehyde (GA) was added as a cross-linkage agent in the HAp/COL slurry after coprecipitation reaction. The reaction of GA in the collagen matrix is highly heterogeneous and complicated (Olde Damink et al., 1995).

*Corresponding author. E-mail: m.kashani@iust.ac.ir.

Zinc is naturally present in bone (Jallot et al., 1999) and stimulates bone growth and bone mineralization (Yamaguchi et al., 1986, 1987, 1988). Zinc has a direct effect on osteoblastic cells in vitro (Hashizume and Yamaguchi, 1993), a potent inhibitory effect on osteoclatic bone resorption (Kishi and Yamaguchi, 1994) and is also known to modify the production of cytokines (Bao et al., 2003). Zinc is an essential trace element having stimulatory effects on bone formation in vitro and in vivo and must be released slowly from the implant because zinc at an elevated level induces adverse reactions.

For the slow release of zinc, β-TCP is one of the most adequate zinc carriers. β-TCP crystal structure has an atomic site, known as a Mg site, that can incorporate divalent cations with an ionic radius ranging from 0.060 to 0.080 nm (Schroeder et al, 1977; Atsu et al., 2002). The ionic radius of zinc is 0.075 nm. β-TCP ceramics are highly biocompatible and resorb slowly in bone tissue.

Generally the uses of composites for bone biomaterials have included three broad areas: functionally graded composites, polymer-ceramic composites (with and without fiber reinforcements) and biomimetic composites or composites with biological macromolecules (Kalpana 2004). The biological process generates highly ordered materials with hybrid composition, complex texture, and ultra-fine crystallites through hierarchical self-assembly. Therefore, it is believed that making of nanocrystal grafts with certain features of natural bone either compositionally or structurally using biomimetic self-assembly may replicate the natural process. This method involves a bottom-up approach, which begins by designing and synthesizing molecules that have the ability to self-assemble or self-organize spontaneously into a higher order of microscale or macroscale structure (Stupp and Brawn, 1997; Stupp et al., 1997).

Biomimetic processing is based on the idea that biologic systems store and process information at the molecular level. The extension of this concept to the processing of synthetic bone and other synthetic tissues has increased in the last few years. A biomimetic nanocrystal is described in such that it can be used as a replacement material for a variety of body applications. The biomimetic nanocrystal includes a fully intermixed and nearly uniformly dispersed composition including hydroxyapatite nanocrystals, gelatin fibers and a polymer. The biomimetic nanocrystal can also be used in a wide range of tissue engineering applications. The biomimetic nanocrystal can be made in scaffolds, which can deliver cells, growth factors and other additives to a healing site. This can be used to regenerate bone, cartilage and other tissues (Ko et al., 2007).

In the present paper, studies of synthesis of HAp with small additions of zinc and cross linked with GA, are reported. In addition, the composites were extensively characterized by SEM/EDX, FT-IR and XRD for morphology, composition and crystallinity evaluation.

MATERIALS AND METHODS

Synthesis of hydroxyapatite/gelatin nanocrystal

The slurry for HAp/GEL composite was prepared by the simultaneous titration method. The amount of $Ca(OH)_2$(Merck) and H_3PO_4(85%, Merck) was calculated to make 10 g of HAp. A homogeneous suspension that included $Ca(OH)_2$ dispersed in 21 ml of DI (deionized) water and an aqueous H_3PO_4 solution with 5 g of GEL(Fluka, From Porcine Skin) was gradually added to the reaction vessel. After the coprecipitation reaction, the total volume was adjusted as 41 ml. The temperature and pH of the reaction solution in the vessel was maintained at 38°C and 8.0, respectively. The reaction temperature was controlled by a water bath. After the reaction, the HAp/GEL slurry was aged at 38°C for 24 h. The precipitated HAp/GEL slurry was filtered and washed 5 times for 1 h with DI water. The final composite was naturally dried at 25°C in the air (Masanori et al., 2001).

Preparation and cross-linkage of hydroxyapatite/gelatin nanocrystals

After the reaction, the obtained slurry was aged at 38°C for 24 h. Then, 0.3 g of GA (25%, Merck) was added and the slurry samples were picked up after 2 h (Myung et al., 2003). The precipitated HAp/GEL/GA slurry was filtered and washed 5 times for 1 h with DI water. The final composite was naturally dried at 25°C in the air.

Preparation and cross-linkage of hydroxyapatite/gelatin nanocrystal doped with Zn^{2+}

$ZnCl_2$ (Merck) in the amount of 0.01 M was added the $Ca(OH)_2$ solution and the same steps of the process were followed. The molar ratio (Ca+Zn)/P=1.67 was used to calculate the weight amount of the reagents for the synthesis of 10 g of calcium phosphate doped with Zn^{2+} (Santos et al., 2007). Then, a part of powder was subjected to heat treatment at 900°C for 2 h for SEM observation. The morphologies of the products were observed through scanning electron microscopy (SEM, Cambridge S365). The crystal phase and structure of the products were determined by X-ray powder diffraction (XRD) with Siemens D5000. FT-IR spectra of nanocrystals were measured upon using KBr pellets. The FT-IR spectra were obtained using a Shimadzu-8400S spectrophotometer in the wave number region of 4000 to 400 cm^{-1}.

Determination of crystallite size of nanohydroxyapatites

The crystallite size of HAp nanoparticles was determined using the diffraction peak of the (0 0 2) plane and the Scherrer equation (Barett et al., 1986; Rusu et al., 2005).

$$D = \frac{K\lambda}{\beta \cos\theta} \quad (1)$$

Where D is the average crystallite size, β the corrected full width of the peak at half of the maximum intensity, FWHM (in radians), λ the wavelength of X-ray radiation (0.1540562 nm), K is a constant related to the crystallite shape and is approximately… (?) Lattice parameters (a and c) were calculated from peaks (2 0 0) and (0 0 2), respectively, using the standard HCP unit cell plane spacing relationship (Cullity, 1978):

$$\frac{1}{d^2} = \frac{4}{3}\left(\frac{h^2 + hk + k^2}{a^2}\right) + \frac{l^2}{c^2} \quad (2)$$

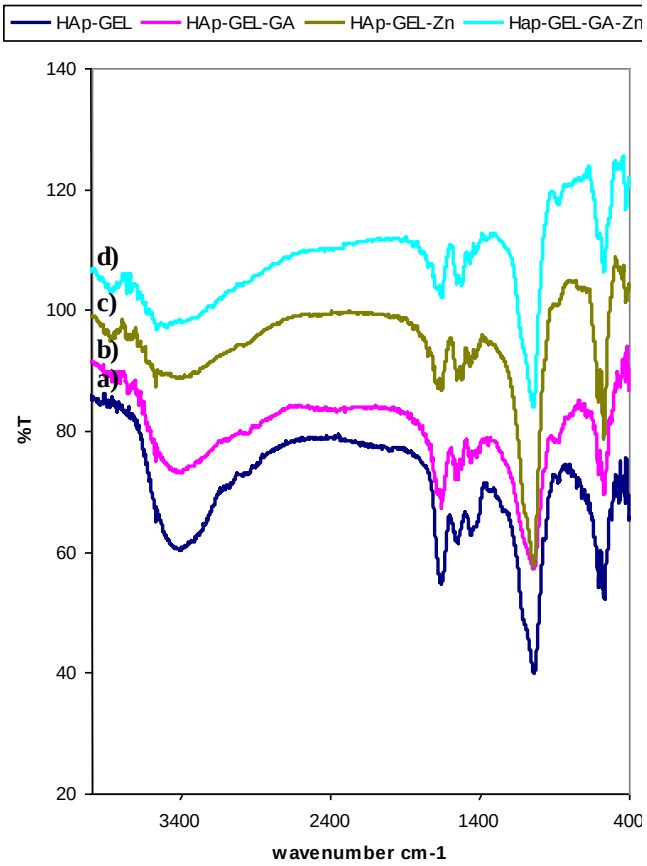

Figure 1. FT-IR spectra for a)HAp/GEL, b)HAp/GEL/GA, c)HAp/GEL/GA/Zn, d)HAp/GEL/GA/Zn compounds.

Where d is the distance between adjacent planes in the set of Miller indices (h k l). The volume (V) of the hexagonal unit cell of each HAp formulation was calculated using the below relation (Webster et al., 2002):

$$V = 2.589a^2c \quad (3)$$

RESULTS AND DISCUSSION

As shown in Figure 1, the FT-IR spectra of nanocrystals are very similar to the spectra of real bone and HAp/COL system? HAp/GEL composite show the typical hydroxyl ion peak at 3568 cm^{-1}, the carbonate mode v2 at 896 cm^{-1}, and the phosphate mode v1; asymmetric mode of phosphate v3 and amide modes as similar to the real bone. The appearance of an amide I mode at 1648 cm^{-1} indicates that HAp/GEL composite adopt a α-helical configuration and this is confirmed by the appearance of amide II mode at 1541 cm^{-1}.

A broad phosphate band in the range from 1200 to 960 cm^{-1} derives from the P-O asymmetric stretching mode (v3) of the PO_4^{3-}group. The broad shape indicates a deviation from the ideal tetrahedral structure of the phosphate ions (Stoch et al., 2000). The triple (v4) and double (v2) degenerated bending modes of O-P-O bonds were found at 604 and 567 cm^{-1} (Frank et al., 2007).

The band at 1339 cm^{-1} in COL is attributed predominantly to the so-called wagging vibration of proline side chains (Meyers et al., 2008). GEL also represents the same band. The red shift of the 1339 cm^{-1} band in GEL has been effectively used to confirm the chemical bond formation between carboxyl ions in GEL and HAp phases. It was observed the typical bands such as N–H stretching at ~3310 cm^{-1} for the amide A, C-H stretching at ~3063 cm^{-1} for the amide B, C-O stretching at 1600 to 1700 cm^{-1} for the amide I, N-H deformation at 1500 to 1550 cm^{-1} for the amide II and N–H deformation at 1200 to 1300 cm^{-1} for the amide III band (Sonju Clasen and Ruyter, 1997; Payne and Veis, 1988; Doyle, 1975; Epaschalis et al., 1997). Normally, the amide I band is strong, the amide II band is weak and the amide III band is moderate.

GA ($OHCCH_2CH_2CH_2CHO$) has two functional groups to be able to link with free amine groups of lysine or hydroxylysine amino acid residues of the polypeptide chains in GEL. All available free amine groups of GEL react with the aldehyde groups of GA to form Schiff bases within 5 min (Olde Damink et al., 1995) and then a large variety of subsequent reactions are involved in the crosslinking of the material (Matsuda et al., 1999; Jakobsen et al., 1983).

It is believed that the red shift in the HAp/GEL system is encouraged by the wagging vibration through the covalent bond formation with Ca^{2+} ions of HAp nanocrystals. It is known that the carboxylic acid groups of GEL at pH>7 are largely ionic in form and offer binding sites for Ca ions because of the ionic attraction (Jakobsen et al., 1983). It should be noted that the hexagonal cell is composed of three primitive cells, brought together at their 120° angles (3 × 120° = 360°). In the case of the hydroxyapatite unit cell, there are four unit cells: two at the 60° angle and two at the 120°(2 × 60° + 2 × 120° =360°) (Meyers et al., 2008). Phase analysis of the XRD patterns of the HAp/GEL/Zn and HAp/GEL/GA/Zn nanocrystals detected different calcium phosphates in the diffraction patterns. A second phase appears when the added cation went into the nanocrystals (Figures 2 and 3). The additional peaks in the patterns indicated presence of the new phases in the HAp lattice consisting mainly of tricalcium phosphate (TCP). TCP has a Ca/P ratio of 1.5 (in comparison to 1.67 for HAp).

Zn^{2+} is known to have an inhibitory effect on HAp formation and to reduce the crystallinity of Hap (LeGeros, 1991; de Groot, 1983). β-$Ca_3(PO_4)_2$ crystallizes in a rhomobohedral unit cell with space group R3c. In pure β-$Ca_3(PO_4)_2$ (Jallot et al., 1999), Ca^{2+} ions are distributed between five crystallographic sites. Four of them are completely filled, the Ca(4) site is only half occupied. The environment of the cations is such that Ca(1), Ca(2) are

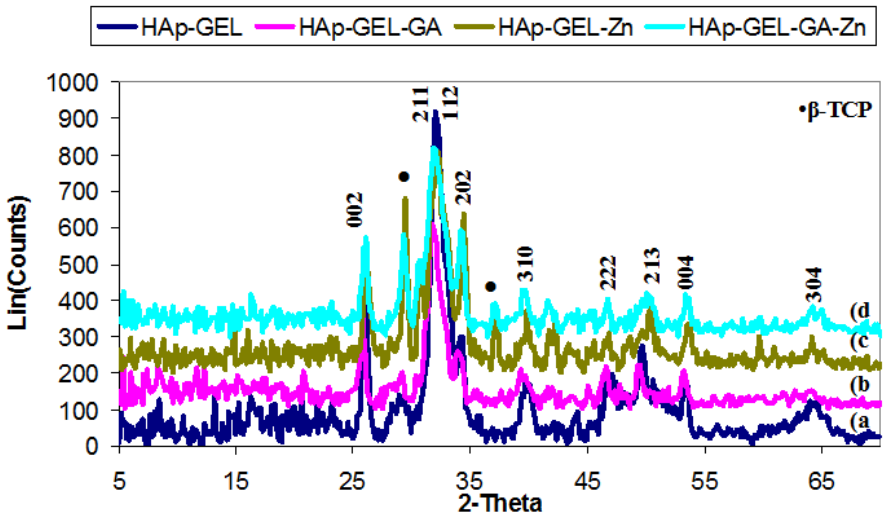

Figure 2. XRD patterns of a) HAp/GEL, b) HAp/GEL/GA, c) HAp/GEL/Zn, d)HAp/GEL/GA/Zn compounds.

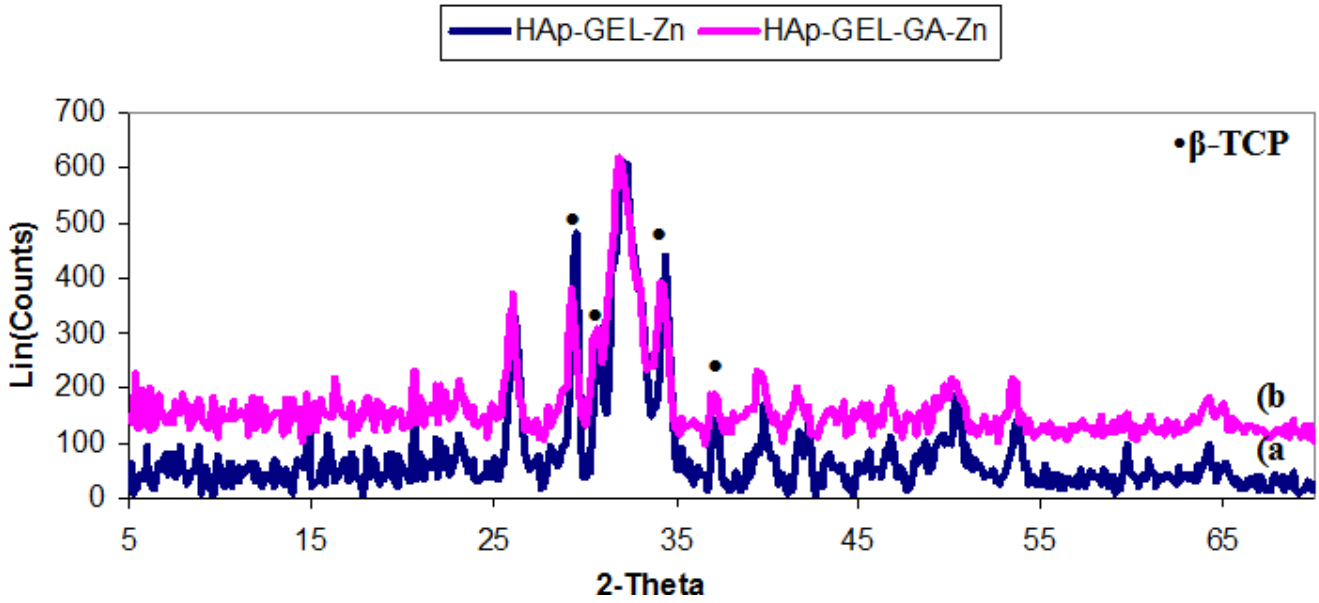

Figure 3. XRD patterns of a) HAp/GEL /Zn , b) HAp/GEL/GA/Zn compounds.

seven and Ca(3) eight coordinated to oxygen atoms. Ca(4) is six coordinated, similar to Ca(5), whose environment is nearly octahedral, however, with only a small axial (trigonal) distortion component.

Mayer et al. (2008) reported that the Mn^{2+} ions occupy the hexacoordinated Ca(5) site solely. The change in the average crystallite size of HAp/GEL and HAp/GEL/GA, HAp/GEL/Zn, HAp/GEL/GA/Zn nanocrystals are shown in Table 1, as determined with the Scherrer equation. Using the (002) plane when the HAp is synthesized by simultaneous titration, its ultimate particle size is around 36 nm.

Lattice parameter information was also obtained from the XRD spectrums. Standard lattice parameter values of a HAp hexagonal crystal, a and c, are 9.44 and 6.88Å, respectively, according to JCPDS 9-432. The HAp/GEL synthesized by simultaneous titration is close to HAp.

Atsu et al. (2002) reported that the growth of the c-face proceeded in a multiple two- dimensional nucleation mode with no spiral growth being observed regardless of the presence of zinc or magnesium, and zinc reduced the diameter of the two-dimensional nuclei more effectively than magnesium.

The HAp structure shrank in volume and lattice parameters of HAp/GEL/Zn and HAp/GEL/GA/Zn nanocrystals were smaller than in pure HAp. Because the

Table 1. Lattice parameters, unite cell volume and size of nanocrystals.

Nanocrystal	Lattice parameters (Å)		Unite cell volume(Å^3)	Size(nm)
	a	*c*		
Hap	9.44	6.88	1587.32	-
HAp/GEL	9.3	6.86	1559.13	36
HAp/GEL/GA	9.01	6.67	1442.62	38
HAp/GEL/Zn	8.9	6.81	1396.56	33
HAp/GEL/GA/Zn	8.9	6.86	1406.81	34

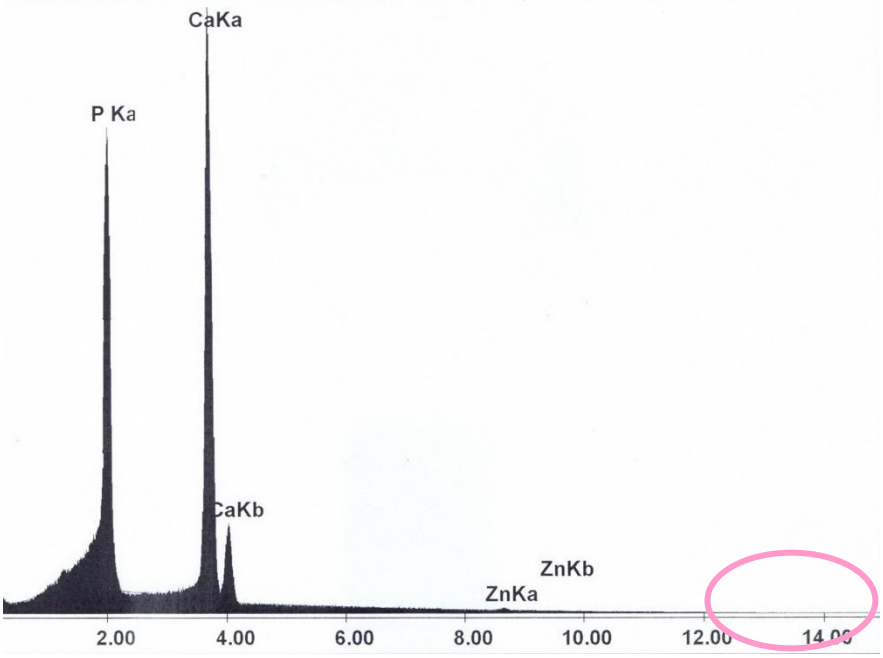

Figure 4. EDX spectrum of HAp/GEL/Zn compounds.

cation Zn is smaller than calcium ions, it is reasonable that their substitution for calcium resulted in a shrinkage of the apatite structure.

Ionic radius of Zn^{2+} with a 6-coordination number with oxygen is 0.72Å, compared with 1.00Å for Ca (Shannon, 1976). Changes in overall volume may imply that dopant substituted for calcium in the HAp lattice since cations smaller than calcium corresponded with shrinkage in crystal volume. These results are consistent with previous work by Ergun et al. (2002), which concluded that Mg^{2+}, Zn^{2+}, and Y^{3+} substitute for calcium in the HAp lattice.

The EDX analysis of the HAp powders resulted in higher concentration of P and Ca elements. The EDX spectrum of HAp/GEL/Zn (Figure 4) showed the presence of zinc peaks, determining the presence of this element in the material constitution. Therefore, the results have given evidence that zinc (as Zn^{2+}) has been successfully incorporated into composite.

It is well known that the rate of mineral formation in bone biology is highly dependent on factors such as pH, the concentration of calcium, phosphate as well as other physiological ions. The carboxyl ion can be an especially active site for the coordination of calcium ions to form ion complexes. These complexes can further interact with PO_4^{3-} ions. It is noted that HAp sample prepared without GEL shows a good crystallinity, but the preferred (002) orientation is not readily apparent. The preferred orientation is greatly enhanced in the HAp/GEL composite system. That is, GEL molecules in the batch induced the strongly preferred development of (002) plane in HAp crystals. GEL macromolecules appear to have a regulatory function for crystal formation. It is known that (002) axis of HAp nanocrystals in bone is associated and aligned with the collagenous matrix in that they are largely arranged with their c axis parallel with the COL fibers. When HAp/GEL/Zn nanocrystal sintered in 900°C, the morphology of HAp particles is clearly rod shape (Figure 5C).

Two crystallographically different Ca sites exist in the

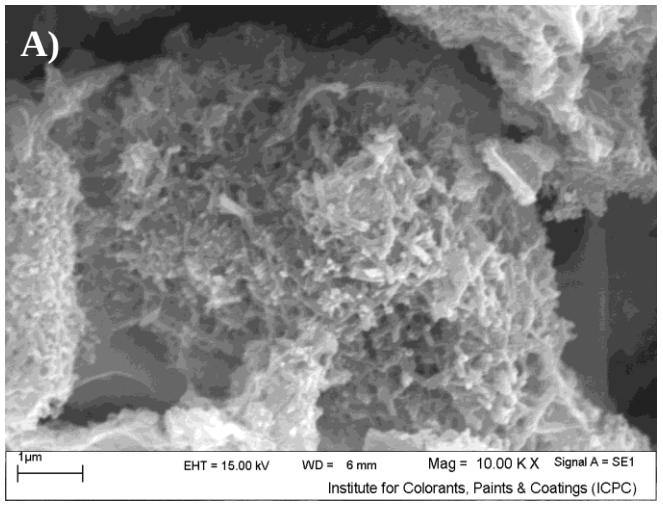

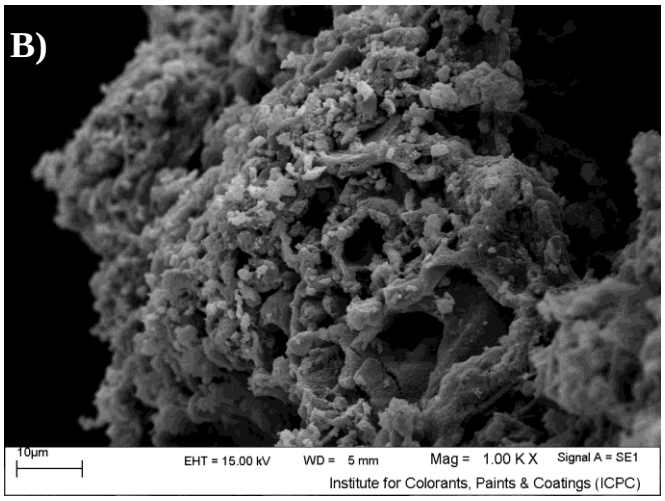

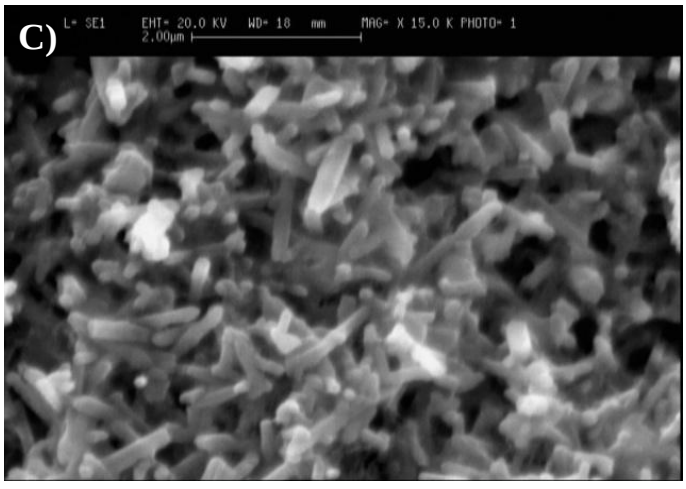

Figure 5. SEM micrographs of A) HAp/GEL, B) HAp/GE/GA, C) HAp/GEL/Zn 900 compounds.

HAp crystal structure. According to the latest study on the HAp structure, Ca(2) appears on the terminated surface of HAp crystals. The Ca(2) has a coordination number of 7, and is strictly held in the structure. On the surface, 2 coordinates of Ca(2) perpendicular to c-axis are lost, which allows to interact with dissociated carboxyl groups on the collagen surface via strict direction. The carboxyl groups, of course, can rotate freely; however, the carboxyl group direction is determined perpendicular to the collagen molecule when the interaction between the carboxyl group and the next Ca(2) on the same HAp crystal occurs. This mechanism obviously results in paralleling of the long axis of a collagen molecule to the c-axis of Hap (Masanori et al., 2004).

It can confirm that this method induces self-assembly mechanism. We believe this is a good evidence of self-assembly of apatitic nanocrystals in GEL matrix. Different nanocrystals of hydroxyapatite-gelatin, HAp/GEL/ Glutaraldehyde, HAp/GEL/Zn and HAp/GEL/GA/Zn were prepared using the biomimetic process. When HAp/ GEL/Zn nanocrystals sintered in 900°C, the morphology of HAp particles is clearly rod shape. It is confirmed that this method induces self-assembly mechanism.

ACKNOWLEDGEMENT

This work was supported financially by The Research council of Iran university of Science and Technology.

REFERENCES

Atsu I, Haruo K, Makoto O, Masako I, Hajime O, Kunio I, Kazuo O, Noriko K, Yu S, Noboru I (2002). Zinc-releasing calcium phosphate for stimulating bone formation. Mater. Sci. Eng. C., 22: 21.

Bao B, Prasad AS, Beck FW, Godmere M (2003). Zinc modulates mRNA levels of cytokines. Am. J. Physiol. Endocrinol. Metab., 285: E1095.

Barett CS, Cohen JB, Faber J, Jenkins R, Leyden DE, Russ JC, Predecki PK (1986). Advances in X-ray Analysis, Plenum Press, New York, 29: 624.

Carotenuto G, Spagnuolo G, Ambrosio L, Nicolais L (1999). Macroporous hydroxyapatite as alloplastic material for dental applications. J. Mater. Sci. Mater. Med., 10: 671.

Chang MC, Ikoma T, Kikuchi M, Tanaka J (2001). Preparation of a porous hydroxyapatite/collagen nanocrystal using glutaraldehyde as a cross-linkage agent. J. Mater. Sci. Lett., 20: 1109.

Chang MC, Ikoma T, Kikuchi M, Tanaka J (2002). The cross-linkage effect of hydroxyapatite/collagen nanocrystals on a selforganization phenomenon. J. Mater. Sci. Mater. Med., 13: 993.

Cullity BD (1978). Elements of X-ray diffraction. 2nd ed.Reading, MA: Addison-Wesley.

De Groot K (1983). Bioceramics of calcium phosphate. FL, USA: CRC Press.

Doyle BB (1975). Infrared spectroscopy of collagen and collagen-like polypeptides. Biopolymers, 14: 937.

Epaschalis EP, Betts E, DiCarlo E, Mendelsohn R, Boskey AL (1997). FTIR microspectroscopic analysis of normal human cortical and trabecular bone. Cacif Tissue Int., 61: 480.

Ergun C, Webster TJ, Bizios R, Doremus RH (2002). Hydroxyl apatite with substituted magnesium, zinc, cadmium, and yttrium I: structure and microstructure. J. Biomed. Mater. Res., 59: 305.

Frank AM, Lenka M, Daniel C, Egle C (2007). Preferred growth orientation of biomimetic apatite crystals. J. Crystal Growth, 304: 46.

Gineste L, Gineste M, Ranz X, Ellefterion A, Guilhem A, Rouquet N, Frayssinet P (1999). Degradation of hydroxyapatite, fluoroapatite, and fluorohydroxyapatite coatings of dental implants in dogs. J.

Biomed. Mater. Res., 48: 224.
Hashizume M, Yamaguchi M (1993). Stimulatory effect of beta-alanyl-Lhistidinato zinc on cell proliferation is dependent on protein synthesis in osteoblastic MC3T3-E1 cells. Mol. Cell Biochem., 122: 59.
Itoh S, Kikuchi M, Koyama Y, Takakuda K, Shinomiya K, Tanaka J (2002). Development of an artificial vertebral body using a novel biomaterial, hydroxyapatite/collagen composite. Biomaterials, 23: 3919.
Jakobsen RJ, Brown LL, Hutson TB, Fink DJ, Veis A (1983). Intermolecular interactions in collagen self-assembly as revealed by Fourier Transform Infrared Spectroscopy. Science, 220 1288.
Jallot E, Irigaray JL, Oudadesse H, Brun V, Weber G, Frayssinet P (1999). Resorption cinetics of four hydroxyapatite-based ceramics by PIXE and neutron activation analysis. Eur. Phys. J. AP., 6: 205.
Kalpana KS (2004). Colloids and Surfaces B: Biointerfaces, 39: 133.
Kikuchi M, Suetsugu Y, Tanaka J, Itoh S, Ichinose S, Shinoyama K, Hiraoka Y, Mandai Y, Nakatani S (1999). The biomimetic synthesis and biocompatibiloty of self-organized hydroxyapatite/collagen composites. Bioceramics, 12: 393.
Kishi S, Yamaguchi M (1994). Inhibitory effect of zinc compounds on osteoclast-like cell formation in mouse marrow cultures. Biochem. Pharmacol., 48: 1225^{-1}230.
Ko C, Chang MC, Douglas W, Hu W (2007). Biomimetic nanocrystal, Pub. No. WO/2007/040574.
Le Geros RZ (1991). Calcium phosphates in oral biology and medicine. New York, USA: Karger.
Mann S, Ozin GA (1996). Synthesis of inorganic materials with complex form. Nature, 365: 499.
Santos MH, Heneine LGD, Mansur HS (2007). Synthesis and characterization of calcium phosphate/collagen biocomposites doped with Zn^{2+}. Mater. Sci. Eng. C., 28: 563.
Masanori K, Soichiro I, Shizuko I, Kenichi S, Junzo T (2001). Self-organization mechanism in a bone-like hydroxyapatite/collagen nanocrystal synthesized *in vitro* and its biological reaction *in vivo*. Biomaterials, 22:1705.
Masanori K, Toshiyuki I, Soichiro I, Hiroko NM, Yoshihisa K, Kazuo T, Kenichi S, Junzo T (2004). Biomimetic synthesis of bone-like nanocrystals using the self-organization mechanism of hydroxyapatite and collagen. Comp. Sci. Technol., 64: 819.
Matsuda S, Iwata H, Se N, Ikata Y (1999). Bioadhesion gelatin films cross-linked with glutaraldehyde. J. Biomed. Mater. Res., 45: 20.
Mayer I, Cohen S, Gdalya S, Burghaus O, Reinen D (2008). Crystal structure and EPR study of Mn-doped β-tricalcium phosphate. Mater. Res. Bull., 43: 447.
Murugan R, Ramakrishna S (2005). Development of nanocrystals for bone grafting. Comp. Sci. Technol., 65: 2385.
Myung CC, Ching-Chang K, William HD (2003). Preparation of hydroxyapatite-gelatin nanocrystal. Biomaterials, 24: 2853.
Olde-Damink LHH, Dijkstra PJ, Van Luyn MJA, Van Wachem PB, Nieuwenhuis P, Feijen J (1995). Glutaraldehyde as a crosslinking agent for collagen-based biomaterials. J. Mater. Sci. Mater. Med., 6: 460.
Payne KJ, Veis A (1988). Fourier transform IR spectroscopy of collagen and gelatin solutions: deconvolution of the amide I band for conformational studies. Biopolymers, 27: 1749.
Rusu VM, Ng CH, Wilke M, Tiersch B, Fratzl P, Peter MG (2005). Size-controlled hydroxyapatite nanoparticles as self-organized organic–inorganic composite materials. Biomaterials, 26: 5414.
Schroeder LW, Dickens B, Brown WE (1977). Crystallographic studies of the role of Mg as a stabilizing impurity in β-$Ca_3(PO_4)_2$: II. Refinement of Mg-containing h-$Ca_3(PO_4)_2$. J. Solid State Chem., 22: 253.
Shannon RD (1976). Crystal Physics, Diffraction, Theoretical and General Crystallography. Acta Cryst., A32: 751.
Sonju-Clasen AB, Ruyter IE (1997). Quantitative determination of type A and type B carbonate in human deciduous and permanent enamel by means of Fourier transformation infrared spectroscopy. Adv. Dent. Res., 11: 523.
Stoch A, Jastrzebski W, Brozek A, Stoch J, Szatraniec J, Trybalska B (2000). FTIR absorption-reflection study of biomimetic growth of phosphates on titanium implants. J. Mol. Struct., 555: 375.
Stupp SI, Braun PV (1997). Molecular manipulation of microstructures: biomaterials, ceramics, and semiconductors. Science, 277: 1242.
Stupp SI, LeBonheur V, Walker K, Li LS, Huggins KE, Keser M, Amstutz A (1997). Supramolecular materials: self-organized nanostructures. Science, 276: 384.
Van BCA, Grote JJ, Kuijpers W, Daems WT, de Groot KA (1986). Macropore tissue ingrowth: a quantitative and qualitative study on hydroxyapatite ceramic. Biomaterials, 7: 137.
Webster TJ, Ergun C, Doremus RH, Bizios R (2002). Hydroxyl apatite with substituted magnesium, zinc, cadmium, and yttrium II: mechanisms of osteoblast adhesion. J. Biomed. Mater. Res., 59: 312.
Yamaguchi M, Inamoto K, Suketa Y (1986). Effect of essential trace metals on bone metabolism in weanling rats: comparison with zinc and other metals' actions. Res. Exp. Med., 186: 337.
Yamaguchi M, Oishi H, Suketa Y (1987). Stimulatory effect of zinc on bone formation in tissue culture. Biochem Pharmacol. Biochem. Pharmacol., 36: 4007.
Yamaguchi M, Oishi H, Suketa Y (1988). Zinc stimulation of bone protein synthesis in tissue culture. Activation of aminoacyl-tRNA synthetase. Biochem. Pharmacol., 37: 4075.